



Simulation of Arc Root Fluctuation in a DC Non-Transferred Plasma Torch with Three Dimensional Modeling

R. Huang, H. Fukanuma, Y. Uesugi, and Y. Tanaka

(Submitted August 25, 2011; in revised form October 20, 2011)

It is well known that the coating quality of plasma spraying is strongly influenced by the instability of jets in the plasma spray, which is due to arc root fluctuation. Three dimensional (3D) unsteady-state modeling was employed in this research to analyze the arc root fluctuation in a DC non-transferred plasma torch. Numerical calculations on the distributions of gas temperature and velocity in the plasma torch were carried out using argon as the plasma gas. The electrical current density and potential were also discussed. The results indicate that the fluctuation of arc inside the plasma torch is mainly induced by the movement of the arc root on the anode surface. The arc root moves downstream with the flow of gas, and simultaneously the arc is bent by electromagnetic force. When the arc bends close enough to the anode boundary, a new arc root is formed somewhere upstream of the current attachment. In this paper the nature of the arc root fluctuation is presented, and also it is demonstrated that the voltage-drop calculated is larger than that measured experimentally because the plasma inside the torch has some deviation from the local thermodynamic equilibrium state hypothesis used in the current study.

Keywords arc root fluctuation, local thermodynamic equilibrium, non-transferred plasma torch, plasma arc

1. Introduction

Plasma spraying is the injection of metal or ceramic powder into hot gas plasma which melts and projects the molten droplets at high velocity onto a substrate to form coatings. Gas molecules, such as argon or hydrogen, dissociate and recombine, producing an extremely hot, high velocity plasma stream inside a torch (Ref 1). Plasma spraying, one of the most widely used in industrial fields based on thermal plasmas, is commonly employed to provide coatings for protection of materials against wear, erosion, corrosion, and thermal loads. Despite its versatility, the limited reproducibility of the process is a major limitation for its wider application. A major factor for this limited reproducibility is the lack of understanding and

control of the dynamic behavior of the arc inside the spraying torch, and the effect of erosion of the anode on the behavior of the plasma jet (Ref 2–6).

A conventional DC non-transferred plasma torch (representing more than 90% of industrial torches) with a stick type cathode is shown schematically in Fig. 1 (Ref 7, 8). After the working gas enters the torch, it is heated by an electric arc formed between a nozzle-shaped anode and a conical cathode, and ejected as a jet. Particles to be plasma sprayed are fed into the particle inlet, heated and accelerated within the plasma jet by the working gas via the plasma arc. The arc inside the torch has been characterized experimentally (Ref 4, 6, 9) and numerically (Ref 1–3, 8). Unfortunately, experiments have been limited by the necessity of high cost equipment and lack of understanding of the results obtained.

Fortunately, numerical calculation provides a valid way to understand arc behavior inside the plasma torch. The modeling of DC arc plasma torches is an extremely challenging task because the plasma flow is highly nonlinear and presents strong property gradients. It is characterized by a wide range of time and length scales, and often includes chemical and thermodynamic non-equilibrium effects, especially near its boundaries (Ref 8). Despite the complexity of the subject, over the past few decades, many papers concerning numerical studies of the characteristics of DC arc plasma torches have been published (Ref 2, 3, 8–22). At the initial stage, a two-dimensional (2D) model was employed in the research to predict the heat transfer and flow patterns inside the plasma torch (Ref 10–14). The predicted arc voltage of the torch in the turbulent regime is much higher than the measured value; in addition the predicted axial location of the arc attachment at the anode surface is also much farther downstream than that

This article is an invited paper selected from presentations at the 2011 International Thermal Spray Conference and has been expanded from the original presentation. It is simultaneously published in *Thermal Spray 2011: Proceedings of the International Thermal Spray Conference*, Hamburg, Germany, September 27–29, 2011, Basil R. Marple, Arvind Agarwal, Margaret M. Hyland, Yuk-Chiu Lau, Chang-Jiu Li, Rogerio S. Lima, and André McDonald, Ed., ASM International, Materials Park, OH, 2011.

R. Huang and **H. Fukanuma**, Plasma Giken Co., Ltd., Tokyo, Japan; and **Y. Uesugi** and **Y. Tanaka**, Kanazawa University, Kanazawa, Japan. Contact e-mail: rz_huang@plasma.co.jp.

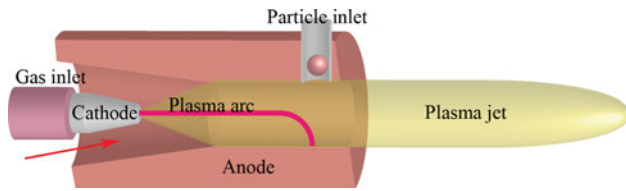


Fig. 1 Schematic of a conventional DC arc spray torch

observed in experiments (Ref 15). With the rapid development of computer technology, the calculation of heat transfer and fluid flow for a 3D thermal plasma torch with axisymmetrical geometries became feasible (Ref 2, 3, 15–22). The models most frequently used for simulations of plasma spray torches rely on the local thermodynamic equilibrium (LTE) approximation, and regard the plasma flow as a property-varying electromagnetic reactive fluid in a state of chemical equilibrium, in which the internal energy of the fluid is characterized by the single parameter of gas temperature (Ref 2, 3, 15–21). Selvan et al. developed a steady-state 3D LTE model to describe the temperature and velocity distributions inside a DC plasma torch. Moreover the arc length and radius were also discussed. But the model overestimated the plasma gas temperature near the arc root due to the assumption that all the electric current transferred to the anode only through a fixed arc root (Ref 3, 16). Klinger et al. also developed a steady-state 3D LTE model simulation of the plasma arc inside a DC plasma torch. However, the position of the arc root was determined arbitrarily (Ref 17). With the steady-state 3D LTE models, the temperature and velocity distributions inside a plasma torch, moreover the arc length and power, could be predicted at some level. However, the fluctuation of the plasma arc cannot be determined. A. Vardelle and J. P. Trelles developed a time-dependent 3D LTE model representing the fluctuations of plasma arc (Ref 2, 18–21). In this unsteady-state 3D LTE model, a critical breakdown electric field or voltage was employed as a criterion to determine the arc root attachment at the anode surface. This made the model more complicated so that it became difficult to calculate. In both the steady and unsteady-state 3D LTE models, the calculated voltage drop was larger compared with the experimental ones due to the overestimation of electrical resistance with the hypothesis of LTE, especially in the vicinity of the electrodes. In order to mimic the plasma arc more correctly, a non-equilibrium (NLTE) model was developed for the non-transferred arc plasma torch, which showed better agreement with the experimental results (Ref 22). However, to solve the NLTE model is extremely difficult due to the fact that the two-temperature chemical equilibrium needs to be considered in comparison with the LTE mode.

In this research, an unsteady-state 3D LTE model was developed to mimic the non-transferred DC plasma torch. In contrast to the steady-state 3D LTE model, the fluctuation of the arc can be obtained. In this model, the electric conductivity at the anode vicinity is specified at

a fixed value of 10^4 S/m. The arc root is determined automatically if the arc is close enough to the anode boundary. Therefore, the unsteady-state 3D LTE model used in the current study is simpler than the previous models reported in some references. Using the current simple 3D LTE model, the plasma gas temperature and velocity distributions were obtained. The fluctuation of the arc inside the torch is also presented.

2. Description of the Mathematical Model

2.1 Model Assumptions

The model developed in this study is based on the following main assumptions for simulating the heat transfer and flow patterns inside a plasma torch.

- (1) The continuum assumption is valid and the plasma can be considered as a compressible, perfect gas in Local Thermodynamic Equilibrium state.
- (2) The plasma is optically thin.
- (3) Gravitational effect and viscous dissipation are considered negligible.
- (4) The induced electric field is negligible in comparison with the applied electric field intensity in the plasma arc region.
- (5) The transport properties of plasma gas are only determined by the plasma gas temperature.
- (6) Because of the lower electric conductivity near the cold boundary of the electrode, the vicinity of anode (within a distance of 0.1 mm) is artificially considered as a high electrical conductivity of 10^4 S/m, so that a new arc root can be formed if the arc is close enough to the inside surface of the anode.

2.2 Governing Equations

Based on the foregoing assumptions, the governing equations for the 3D time-dependent model for the arc plasma can be written as follows:

Conservation of mass:

$$\frac{\partial \rho}{\partial t} + \nabla \cdot (\rho \vec{V}) = 0$$

Conservation of momentum:

$$\rho \left(\frac{\partial \vec{V}}{\partial t} + \vec{V} \cdot \nabla \vec{V} \right) = \vec{j} \times \vec{B} - \nabla \left[P + \frac{2}{3} \mu (\nabla \cdot \vec{V}) \right] + 2 \nabla \cdot (\mu \vec{S})$$

Conservation of energy:

$$\rho c_p \left(\frac{\partial T}{\partial t} + \vec{V} \cdot \nabla T \right) - \frac{DP}{Dt} = \vec{j} \cdot \vec{E} - S_r + \nabla \cdot (\lambda \nabla T)$$

Maxwell electromagnetism equations:

$$\nabla \cdot (-\sigma \nabla \phi) = 0$$

$$\vec{E} = -\nabla\phi$$

$$\nabla^2\vec{A} = -\mu_0\vec{j}$$

$$\vec{B} = \nabla \times \vec{A}$$

Ohm law:

$$\vec{j} = \sigma\vec{E}$$

where ρ is gas mass density, t time, \vec{V} velocity, \vec{j} electric current density, \vec{B} magnetic induction vector, P gas pressure, μ dynamic viscosity, \vec{S} strain rate tensor, c_p specific heat at constant pressure, \vec{E} electric field, S_r volumetric net radiation losses, λ gas thermal conductivity, σ electric conductivity, ϕ electric potential, \vec{A} magnetic vector potential and μ_0 permeability of free space.

For the gas flow calculation, the K - ϵ model is employed in this study. The thermodynamic and transport properties of the plasma gas are taken from Ref 23 and 24.

2.3 Computational Domain and Boundary Conditions

The geometry used in the current study corresponds to the SG-100 plasma torch from Praxair. The computational domain formed by the region inside the torch is limited by the cathode, the gas flow inlet, the anode and the outlet as shown in Fig. 2. The computational domain is meshed using 217600 hexahedral cells with 224567 nodes. For gas flow calculations, the Standard K - ϵ model is employed in this study. The governing equations are solved by FLUENT, commercial CFD software, with the SIMPLE algorithm.

As seen in Fig. 2, the boundary of the computational domain is divided into 4 different faces to allow the specification of boundary conditions. Table 1 shows the

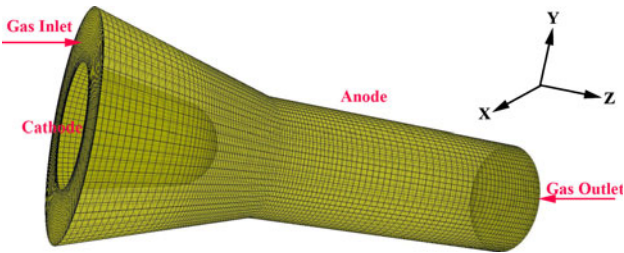


Fig. 2 Geometry of the computational domain

Table 1 Boundary conditions

Boundary	P	V	T	ϕ	A
Inlet	P_{in}	50 SLM	300 K	$\partial\phi_n = 0$	0
Cathode	$\partial P_n = 0$	0	3000 K	$j(r)$	$\partial A_n = 0$
Anode	$\partial P_n = 0$	0	$h_w(T - T_w)$	0	$\partial A_n = 0$
Outlet	1 atm	$\partial V_n = 0$	$\partial T_n = 0$	$\partial\phi_n = 0$	$\partial A_n = 0$

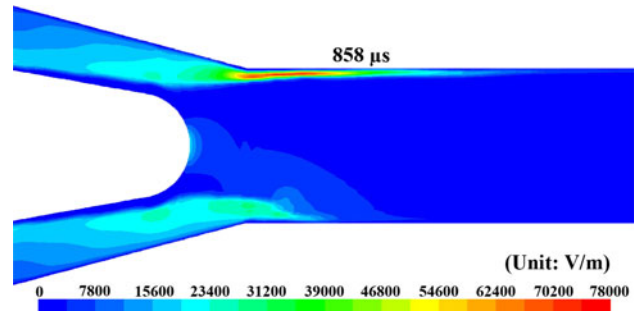


Fig. 3 Electric field strength distribution inside the plasma torch at the time of 858 μ s

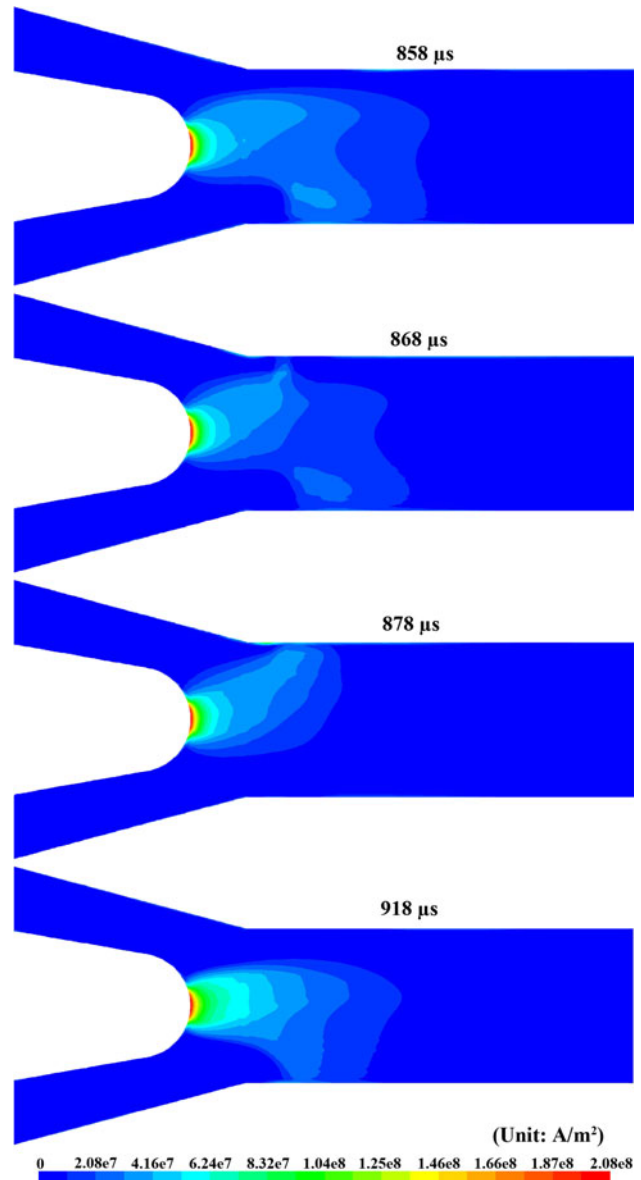


Fig. 4 Electric current distribution inside the plasma torch at different times

boundary conditions used in the simulation, where P_{in} represents the inlet pressure equal to 111325 Pa (10 kPa overpressure), h_w the convective heat transfer coefficient at the anode wall equal to 1×10^5 W/m²/K (Ref 19–22), T_w a reference cooling water temperature of 500 K. The current density of the cathode is defined by:

$$j(r) = J_{cath0} \exp\left(-\left(\frac{r}{R_c}\right)^{n_c}\right)$$

where r is radial distance from the torch axis ($r^2 = x^2 + y^2$), and J_{cath0} and n_c are parameters that specify the shape of current density profile. The R_c is

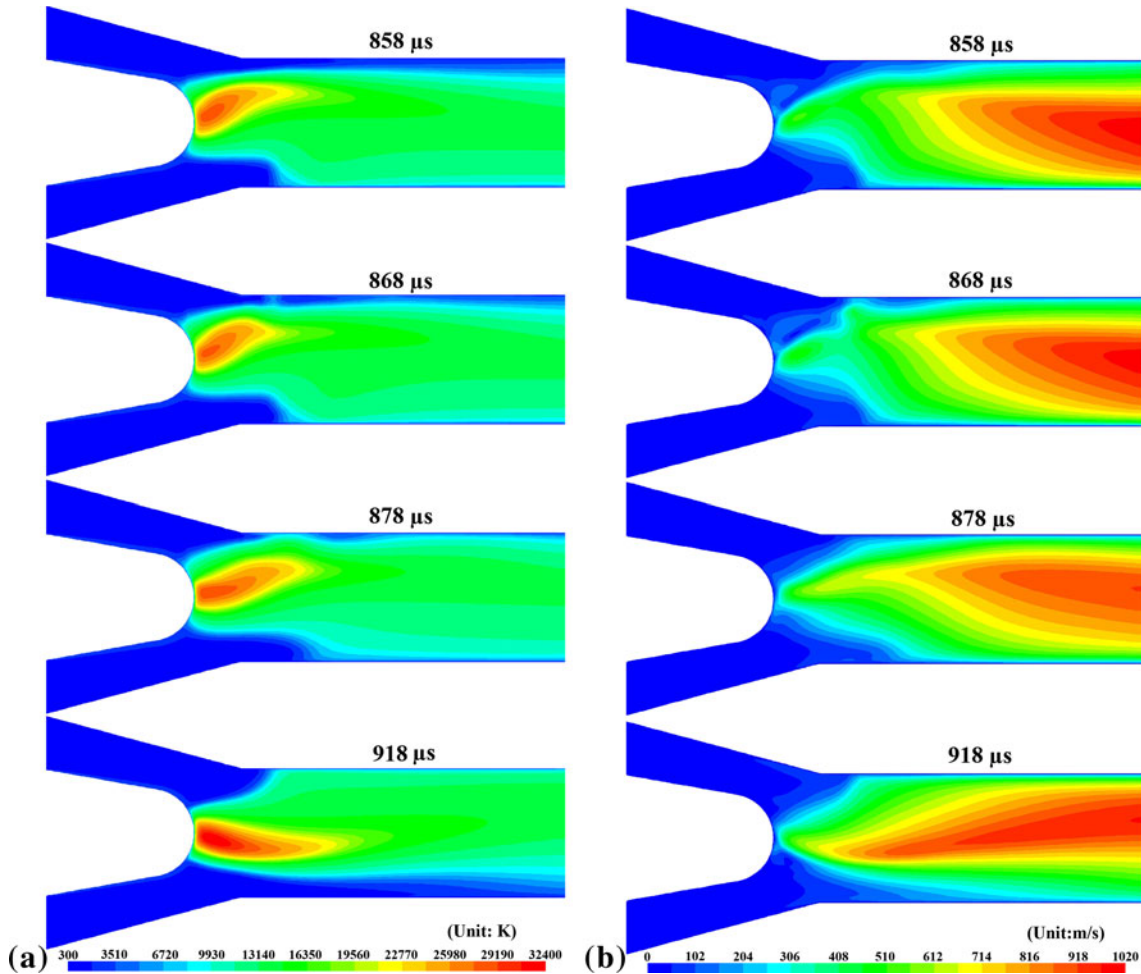


Fig. 5 Plasma gas temperature (a) and velocity (b) distributions inside the plasma torch at different times

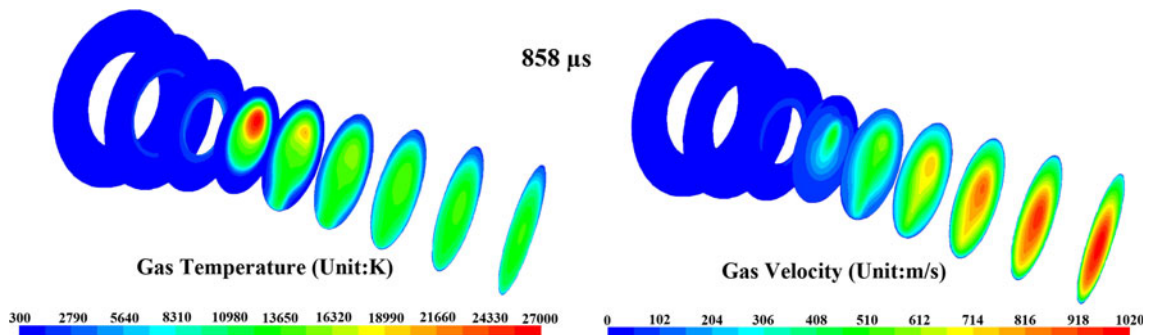


Fig. 6 Plasma gas temperature and velocity distributions inside the torch of different axial cross sections

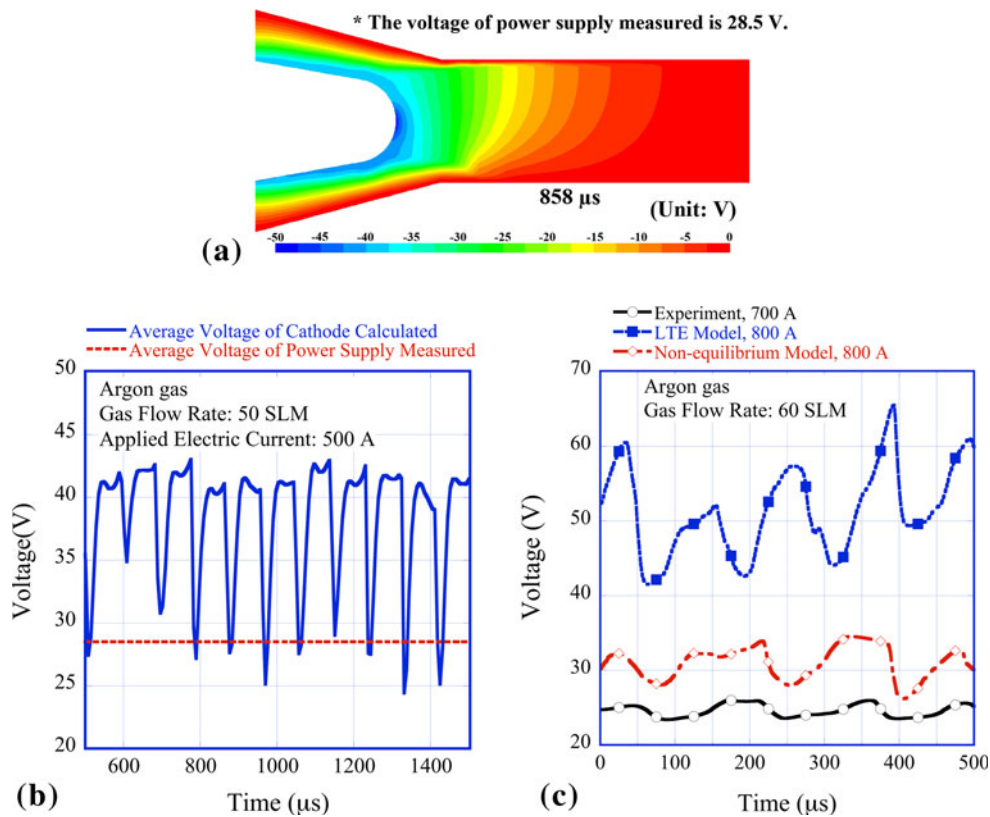


Fig. 7 The electric potential distribution inside the plasma torch (a), the time-evolution of cathode voltage in this study (b) and the cathode voltage reported in Ref 22 by Trelles et al. (c)

calculated to ensure that integration of $j(r)$ over the cathode equals the total applied current. According to Ref 20 and 23, J_{cath0} of $2.08 \times 10^8 \text{ A/m}^2$, n_c of 4 and R_c of 0.913 mm were used in this study for the applied electric current of 500 A.

Argon gas was employed as the plasma gas in this study. As Table 1 shows, the spray conditions are 500 A for the applied electrical current and 50 SLM for the gas flow rate.

3. Results and Discussions

3.1 Flow Fields Inside the Torch

The distribution of electric field strength inside the plasma torch calculated by the LTE model is shown in Fig. 3. The maximum electric field strength is about $0.78 \times 10^5 \text{ V/m}$ near the anode boundary. Figure 4 shows the time-evolution of the electric current distributions. It reveals that the arc root moved downstream for the time of 858-868 μs . At the same time, a new electric current “path” is formed near the maximum electric field area indicated in Fig. 3. It seems that the electric field strength is strong enough to break down the gas gap between the arc and anode boundary to form a new arc root. Consequently, electric current will go through the old arc root and the new one simultaneously. As time elapses, the old

arc root will disappear and only the new one will remain as shown in Fig. 4.

With the arc root movement and transition as Fig. 4 shows, the parameters inside the plasma torch should fluctuate. The time-evolution of gas temperature and velocity distributions inside the plasma torch are shown in Fig. 5. It indicates that the temperature distributions of arc bend and deviate to the contrary side because the electrical current mainly passes through the arc root. The deviation results in a rise of the electric field strength at the fringe of the arc to form an electric field breakdown. When the arc bends close enough to the anode surface and its local electric field is high enough to break down the gap between the arc and anode boundary, a new arc root is formed and the former arc root starts to disappear. As the old arc root disappears, the arc will deviate to the other side too in order to generate the next attachment as shown in Fig. 5(a). The gas velocity distributions inside the plasma torch show that the velocity inside the plasma torch also experiences significant fluctuation with the arc root movement and transition as shown in Fig. 5(b). The fluctuations of plasma gas temperature and velocity are the main causes of plasma jet fluctuation, consequently influencing the reproducibility of coatings. A maximum gas temperature of more than 30000 K and velocity of more than 1000 m/s are obtained under the current spray conditions of argon gas, 500 A electric current and 50 SLM gas flow rate.

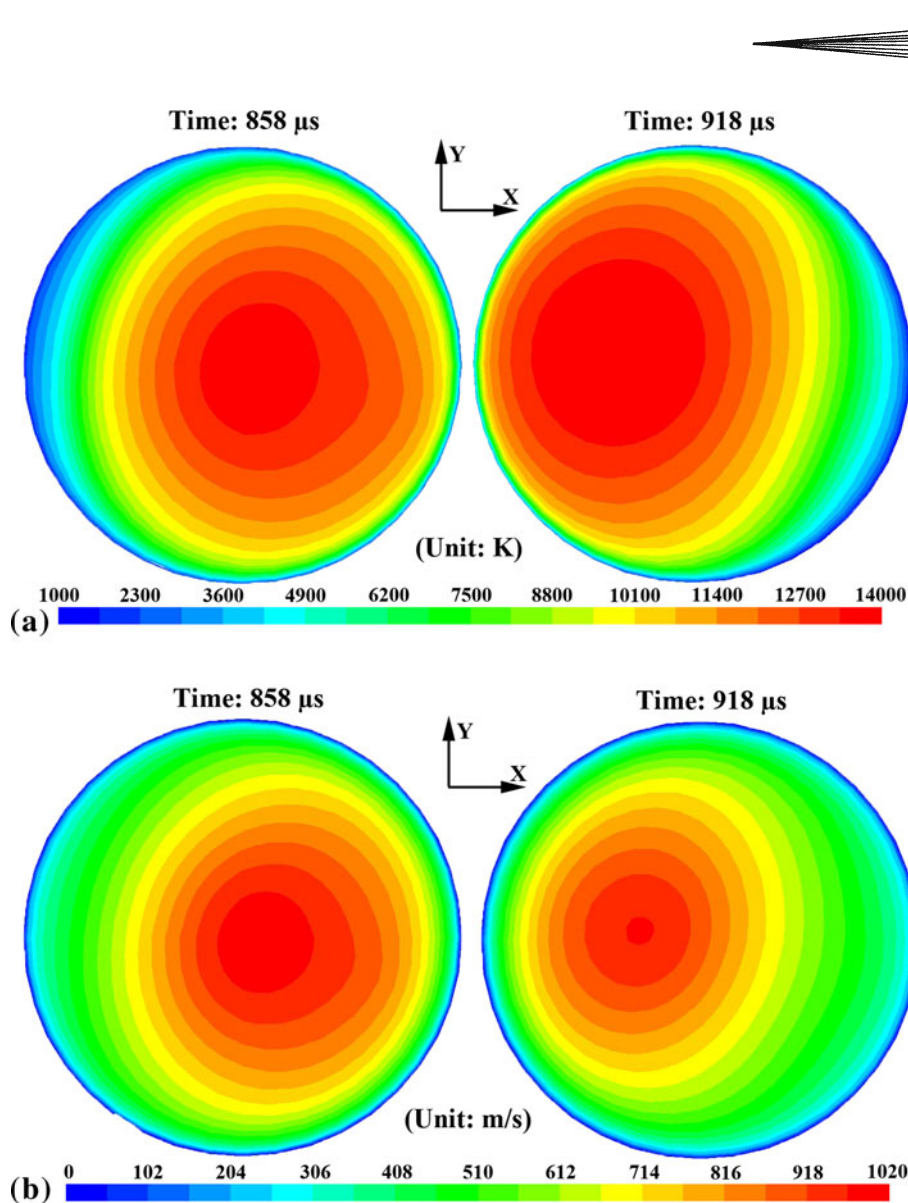


Fig. 8 Plasma gas temperature (a) and velocity (b) distributions at the torch exit

Figure 6 shows the gas temperature and velocity at different cross sections inside the plasma torch. It can be seen that, due to the fluctuations of the arc, the gas temperature and velocity distributions are asymmetric even though the geometry of the plasma torch is axisymmetric.

The electric potential distribution of the plasma arc is shown in Fig. 7(a). The voltage drop of the arc column should theoretically be lower than the voltage of the power supply because of the sheath voltage drop. However, the arbitrary higher electric conductivity nearby the electrodes and LTE assumptions result in lower accuracy for the electric potential distribution especially in the vicinity of the cathode. Therefore, the sheath voltage drop cannot be observed and the voltage drop of the arc column calculated is much higher than the voltage of the power supply measured experimentally. Figure 7(b) shows the time-evolution of the average voltage of the cathode. It reveals the frequency of the plasma arc fluctuation is

about 11 kHz. Compared with the electrode voltage reported in Ref 22 as shown in Fig. 7(c), the electrode voltage calculated in the current study is higher than the ones calculated with the non-equilibrium (NLTE) mode. However, taking into consideration the difference of applied electrical current, it seems that the voltage in the current study approximately agrees with the ones calculated by Trelles et al. using the LTE model.

3.2 Gas Flow at the Torch Exit

The plasma jet is mainly determined by the gas flow at the torch exit. The parameters of the plasma jet can be predicted by the distributions of gas temperature and velocity of the torch outlet. Therefore, it is extremely important to mimic the outlet temperature and velocity of gas in order to understand the fluctuations of the plasma spray jet. The calculated distributions of gas temperature

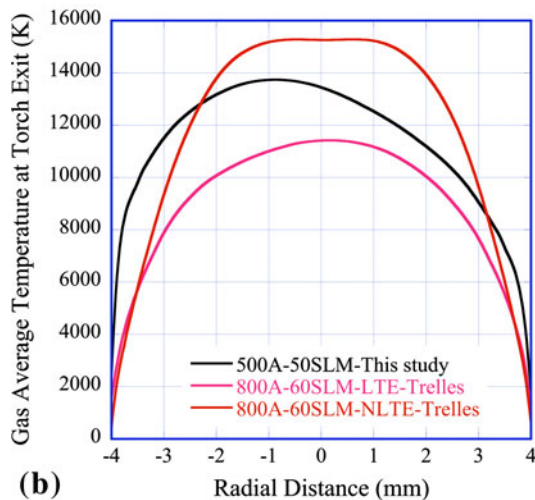
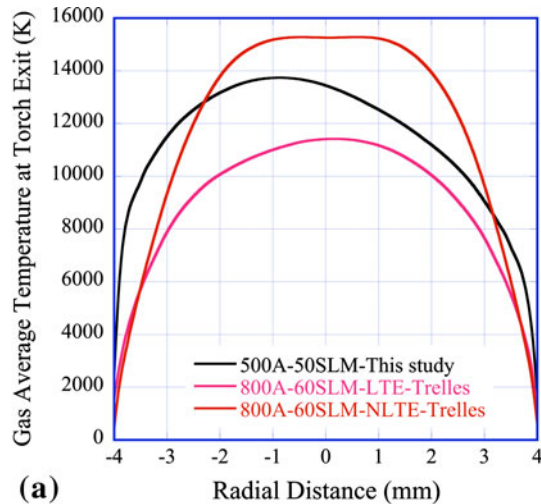


Fig. 9 Plasma gas average temperature (a) and velocity (b) at the torch exit

and velocity at the nozzle exit are shown in Fig. 8. The maximum temperature of about 14000 K and velocity of about 1000 m/s are obtained at the nozzle exit. It can be found that the value calculated agrees well with the results measured experimentally according to Ref 25–27.

Figure 9 shows the average temperature and velocity profiles at the torch exit, which represent the time-averaged values along its x -axis. The temperature and velocity at the torch exit calculated in the current study are probably similar to the values calculated with NLTE model in Ref 22, when taking into consideration the higher electric current as shown in Fig. 9.

Figure 10 presents the gas flow rate at the torch exit. It can be seen that the gas flow rate fluctuates at the torch exit although the inlet gas flow rate is kept constant at 50 SLM. The fluctuation of gas flow rate is caused by the gas velocity fluctuation inside the plasma torch. In spite of the fluctuation, the gas flow rate at the torch exit does not deviate much from the value of 50 SLM due to the conservation of mass.

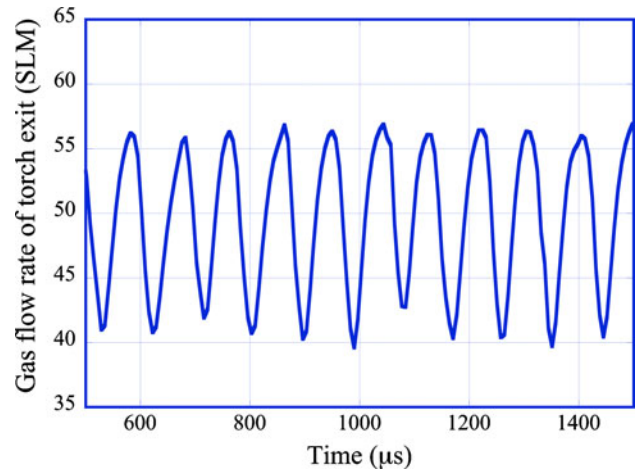


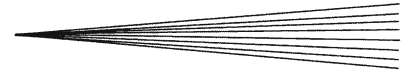
Fig. 10 The time-evolution of gas flow rate to the torch exit

4. Conclusions

A simple LTE model has been developed and applied to the three-dimensional and time-dependent simulation of the flow inside a DC arc plasma torch. As an unsteady-state model, this mode well mimicked the arc fluctuation inside the plasma torch. Despite the simple assumption of higher electrical conductivity in the vicinity of the electrodes, a significant level of accuracy was obtained compared with the experimental and simulation results in the previous reports. Using the simple LTE model, the temperature and velocity distribution of arc gas inside the torch were calculated. The electric current mainly passes through the arc root to the anode. The electric current “path” causes the arc to bend and the electric field strength to rise at the contrary side of the arc root. When the arc is close enough to the anode boundary and the electric field strength is strong enough, then the old arc root will transfer to a new one. The movement and transition of the arc root results in the fluctuation of the plasma arc inside the plasma torch with a frequency of 11 kHz. A gas temperature of about 14000 K and velocity of about 1000 m/s were obtained at the torch exit. A higher voltage drop of the arc column was obtained compared to the one measured experimentally because the LTE assumption underestimated the electric conductivity of plasma gas inside the torch, especially in the regions around the arc root.

References

1. G.V. Miloshevsky, G.S. Romanov, V.I. Tolkach, and I.Yu. Smurov, Simulation of the Dynamics of Two-Phase Plasma Jet in the Atmosphere. *Proceedings of III International Conference on Plasma Physics and Plasma Technology*, Minsk, Belarus, September 18-22, 2000, p 244-247
2. J.P. Trelles, E. Pfender, and J. Heberlein, Multiscale Finite Element Modeling of Arc Dynamics in a DC Plasma Torch, *Plasma Chem. Plasma Process.*, 2006, **26**(6), p 557-575
3. B. Selvan and K. Ramachandran, Comparisons Between Two Different Three-Dimensional Arc Plasma Torch Simulations, *J. Therm. Spray Technol.*, 2006, **18**(5–6), p 846-857



4. Z. Duan and J. Heberlein, Arc Instabilities in a Plasma Spray Torch, *J. Therm. Spray Technol.*, 2002, **11**(1), p 44-51
5. D. Outcalt, M. Hallberg, G. Yang, J. Heberlein, E. Pfender, and P. Strykowski, Instabilities in Plasma Spray Jets, *Thermal Spray 2006: Science, Innovation, and Application* B.R. Marple, M.M. Hyland, Y.-C. Lau, R.S. Lima, and J. Voyer, Ed., May 15–18, 2006 (Seattle, Washington), ASM International, 2006, p 803-807
6. J.F. Coudert, M.P. Planche, and P. Fauchais, Characterization of DC Plasma Torch Voltage Fluctuations, *Plasma Chem. Plasma Process.*, 1996, **16**(1), p 211S-227S
7. P. Fauchais, Understanding Plasma Spraying, *J. Phys. D*, 2004, **37**(9), p R86-R108
8. J.P. Trelles, C. Chazelas, A. Vardelle, and J.V.R. Heberlein, Arc Plasma Torch Modeling, *J. Therm. Spray Technol.*, 2009, **18**(5–6), p 728-752
9. R. Ramasamy and V. Selvarajan, Current-Voltage Characteristics of a Non-Transferred Plasma Spray Torch, *Eur. Phys. J. D*, 2000, **8**(1), p 125-129
10. R. Westhoff, A.H. Dilawari, and J. Szekely, A Mathematical Representation of Transport Phenomena Inside a Plasma Torch, *Mater. Res. Soc. Symp. Proc.*, 1991, **199**, p 213-219
11. R. Westhoff and J. Szekely, A Model of Fluid, Heat Flow, and Electromagnetic Phenomena in a Nontransferred Arc Plasma Torch, *J. Appl. Phys.*, 1991, **70**(7), p 3455-3466
12. H. Peng, Y. Lan, and C. Xi, Modeling of Plasma Jets with Computed Inlet Profiles, *Proceedings of the 13th International Symposium on Plasma Chemistry*, C.K. Wu, Ed., Peking University Press, Beijing, 1997,
13. D.A. Scott, P. Kovitya, and G.N. Haddad, Temperatures in the Plume of a DC Plasma Torch, *J. Appl. Phys.*, 1989, **66**(11), p 5232-5239
14. S. Paik, P.C. Huang, J. Heberlein, and E. Pfender, Determination of the Arc Root Position in a DC Plasma Torch, *Plasma Chem. Plasma Process.*, 1993, **13**(3), p 379-397
15. H.-P. Li and E. Pfender, Three Dimensional Modeling of the Plasma Spray Process, *J. Therm. Spray Technol.*, 2007, **16**(2), p 245-260
16. B. Selvan, K. Ramachandran, K.P. Sreekumar, T.K. Thiagarajan, and P.V. Ananthapadmanabhan, Three-Dimensional Numerical Modeling of an Ar-N₂ Plasma Arc Inside a Non-Transferred Torch, *Plasma Sci. Technol.*, 2009, **11**(6), p 679-687
17. L. Klinger, J.B. Vos, and K. Appert, High-Resolution CFD Simulation of a Plasma Torch in 3 Dimensions, *CRPP-REPORT-2003-024*, LRP 762, http://infoscience.epfl.ch/record/121307/files/lrp_762_03_hq.pdf, 2003
18. C. Baudry, A. Vardelle, G. Mariaux, F.C. Delalondre, and F.E. Meillot, Three-Dimensional and Time-Dependent Model of the Dynamic Behavior of the Arc in a Plasma Spray Torch, *Thermal Spray 2004: Advances in Technology and Applications*, D. von Hofe, Ed., ASM International, Materials Park, 2004, p 717-723
19. E. Moreau, C. Chazelas, G. Mariaux, and A. Vardelle, Modeling the Restrike Mode Operation of a DC Plasma Spray Torch, *J. Therm. Spray Technol.*, 2006, **15**(4), p 524-530
20. J.P. Trelles, E. Pfender, and J.V.R. Heberlein, Modelling of the Arc Reattachment Process in Plasma Torches, *J. Phys. D*, 2007, **40**(18), p 5635-5648
21. J.P. Trelles and J.V.R. Heberlein, Simulation Results of Arc Behavior in Different Plasma Spray Torches, *J. Therm. Spray Technol.*, 2006, **15**(4), p 563-569
22. J.P. Trelles, J.V.R. Heberlein, and E. Pfender, Non-Equilibrium Modelling of Arc Plasma Torches, *J. Phys. D*, 2007, **40**(19), p 5937-5952
23. M.I. Boulos and P. Fauchais, *Thermal Plasmas: Fundamentals and Applications, Vol. I*, Springer, Berlin, 1994
24. V. Colombo, E. Ghedini, and P. Sanibondi, Thermodynamic and Transport Properties in Non-Equilibrium Argon, Oxygen and Nitrogen Thermal Plasmas, *Prog. Nucl. Energy*, 2008, **50**(8), p 921-933
25. S.C. Snyder, G.D. Lassahn, and J.D. Grandy, Direct Determination of Gas Velocity and Gas Temperature in an Atmospheric-Pressure Argon-Hydrogen Plasma Jet, *J. Quant. Spectrosc. Radiat. Transf.*, 2007, **107**(2), p 217-225
26. M.P. Planche, J.F. Coudert, and P. Fauchais, Velocity Measurements for Arc Jets Produced by a DC Plasma Spray Torch, *Plasma Chem. Plasma Process.*, 1998, **18**(2), p 263-283
27. J.-L. Dorier, Ch. Hollenstein, A. Salito, M. Loch, and G. Barbezat, Influence of External Parameters on Arc Fluctuations in a F4 DC Plasma Torch Used for Thermal Spraying, *Thermal Spray 2000: Surface Engineering via Applied Research*, C.C. Berndt, Ed., ASM International, Materials Park, p 37-43